BIOCHEMISTRY
including biophysical chemistry & molecular biology
Article

Biochemistry **2009,** *48,* 8473–8482 8473
DOI: 10.1021/bi900615z

Comparison of the Thermodynamics and Base-Pair Dynamics of a Full LNA:DNA Duplex and of the Isosequential DNA:DNA Duplex†

Gilles Bruylants,[⊥] Marina Boccongelli,[⊥] Karim Snoussi,[‡,#] and Kristin Bartik*,[⊥]

[⊥]*Molecular and Biomolecular Engineering, Service Matières et Matériaux, CP165/64, Université Libre de Bruxelles, 50 Avenue F.D. Roosevelt, 1050 Bruxelles, Belgium, and* [‡]*Department of Chemistry, Université Catholique de Louvain, Bâtiment Lavoisier, Place Louis Pasteur, 1, B-1348 Louvain-la-Neuve, Belgium.* [#]*Current address: Japan Science and Technology Agency, NSEP Aoba Incubation Square, 468-15 Aramaki Aza Aoba, Aobaku, Sendai, Miyagi, 980-0845, Japan.*

Received April 9, 2009; Revised Manuscript Received July 28, 2009

ABSTRACT: Locked nucleic acids (LNA), conformationally restricted nucleotide analogues, are known to enhance pairing stability and selectivity toward complementary strands. With the aim to contribute to a better understanding of the origin of these effects, the structure, thermal stability, hybridization thermodynamics, and base-pair dynamics of a full-LNA:DNA heteroduplex and of its isosequential DNA:DNA homoduplex were monitored and compared. CD measurements highlight differences in the duplex structures: the homoduplex and heteroduplex present B-type and A-type helical conformations, respectively. The pairing of the hybrid duplex is characterized, at all temperatures monitored (between 15 and 37 °C), by a larger stability constant but a less favorable enthalpic term. A major contribution to this thermodynamic profile emanates from the presence of a hairpin structure in the LNA single strand which contributes favorably to the entropy of interaction but leads to an enthalpy penalty upon duplex formation. The base-pair opening dynamics of both systems was monitored by NMR spectroscopy via imino protons exchange measurements. The measurements highlight that hybrid G-C base-pairs present a longer base-pair lifetime and higher stability than natural G-C base-pairs, but that an LNA substitution in an A-T base-pair does not have a favorable effect on the stability. The thermodynamic and dynamic data confirm a more favorable stacking of the bases in the hybrid duplex. This study emphasizes the complementarities between dynamic and thermodynamical studies for the elucidation of the relevant factors in binding events.

Locked nucleic acids (LNA),[1] conformationally restricted nucleotide analogues, constitute an important addition to the tools available for nucleic acid diagnostics and nucleic acid therapeutics. LNA monomers contain a modified ribose moiety in which the 2′O and 4′C are linked by a methylene bridge (2′-O,4′-C-methylene-β-D-ribofuranosyl), locking the sugar in the C3′-endo/N-type conformation (*1*−*3*). LNA resemble natural nucleic acids with respect to Watson−Crick base pairing and the potential of LNA containing oligonucleotides lies in their ability to mediate high affinity pairing with complementary RNA or DNA strands, with equal or often superior sequence specificity than their natural equivalent (*4*−*7*). Various applications and uses of LNA containing oligonucleotides have been reported and discussed in the literature. It has for example been shown that LNA containing oligonucleotides possess a gene silencing potential (*7*−*9*), that they are potential antisense drugs (*10*−*12*), and that they can be advantageously be used as probes in hybridization-based assays such as expression profiling, DNA sequencing, and SNP genotyping (*7*, *13*−*19*). It has furthermore been shown that the introduction of LNA monomers into DNA oligonucleotides ensures substantial serum stability, with low toxicity, which is a prerequisite for any potential therapeutic use (*20*).

Numerous structural and thermodynamic studies have been undertaken on LNA containing duplexes in order to try to elucidate the factors at the origin of the observed increased pairing selectivity and thermal stability. When LNA are incorporated into DNA or RNA:DNA duplexes they maintain a right-handed helix conformation with all the bases in the anti conformation. NMR studies however highlight that the incorporation of LNA monomers into DNA duplexes induces the local acquisition of A-type helix characteristics (*21*−*26*), with an increased N-type contribution to the sugar conformation of the DNA base-pairs adjacent to the incorporated LNA(*23*). The incorporation of LNA nucleotides into the DNA strand of a DNA:RNA hybrid duplex also leads to an increase in the deoxyribose N-type conformation (*22*, *26*). When a full LNA strand is opposed to its cDNA strand the deoxyribose pucker pattern is similar to the one observed in RNA:DNA (*24*). These experimentally observed changes have been reproduced by Molecular Dynamic simulations (*27*, *28*).

The stability of LNA-containing duplexes is generally evaluated via thermal denaturation experiments. The observed increase in the melting temperatures (T_m) of LNA containing duplexes relative to their native reference duplexes, range between +1 and

†G.B. thanks the Belgian "Fonds de la Recherche Scientifique − FNRS" for a postdoctoral fellowship. M.B. thanks the Belgian "Fonds pour la formation à la Recherche dans l'Industrie et dans l'Agriculture" for a Ph.D. grant.

*Corresponding author: Tel.: +32 6502063; fax: +32 6502606; e-mail: kbartik@ulb.ac.be.

[1]Abbreviations: LNA, locked nucleic acids; RNA, ribonucleic acid; DNA, deoxyribonucleic acid; DSC, differential scanning calorimetry; ITC, isothermal titration calorimetry; NMR, nuclear magnetic resonance; CD, circular dichroism.

Published on Web 07/29/2009

+8 °C per LNA monomer introduced into a DNA strand paired to its complementary DNA strand (*1*, *20*, *29*−*35*) and between +2 and +9 °C when paired to its complementary RNA strand (*1*, *29*−*31*, *36*). The observed range of ΔT_m for each LNA nucleotide is however sequence dependent with both 5′ and 3′ unmodified neighbors influencing stability. The increase in T_m saturates for an approximate LNA content of 50% (*4*, *31*). This has been interpreted as a consequence of the ability of LNA monomers to induce A-type characteristics, an effect which reaches a maximum when 50% of the nucleotides are modified (*21*, *23*). The enthalpic ($\Delta H°$) and entropic ($\Delta S°$) contributions to the free energy ($\Delta G°$) characterizing the stability of LNA containing duplexes have in a few cases been extracted from the thermal denaturation data (*2*, *29*, *34*−*38*). A more efficient stacking of the bases in LNA containing duplexes, resulting from the induced A-type helical conformation, is evoked for the origin of a more favorable enthalpic term (*2*, *34*−*36*, *39*). A more favorable entropic term is explained by the restriction of ribose flexibility and also by a favorable preorganization of the LNA containing single strands (*2*, *34*, *39*). The influence of LNA on the stability of 2′-O-methyl RNA/RNA duplexes has also been studied (*39*, *40*), and there too enhanced stacking interactions and helical preorganization of the single-stranded oligonucleotides are reported as contributing to the stabilization of the duplexes.

When thermodynamic parameters are derived from the analysis of denaturation curves, they are obtained at T_m. As $\Delta H°$ and $\Delta S°$ can be strongly temperature dependent a comparison between duplexes is truly meaningful only if these quantities are extrapolated to a common temperature. This requires the knowledge of the ΔC_p of the systems, the difference between the molar heat capacity of the duplex and of the single strands parameter which can in principle be derived from DSC and UV data but rarely with good precision (*41*−*43*). A more precise and complete thermodynamic characterization of duplex formation can be obtained by isothermal titration calorimetry (ITC) which is able to provide, at any given temperature, the complete thermodynamic profile of a complexation process ($\Delta G°$, $\Delta H°$, and $\Delta S°$). By performing experiments at different temperatures, it is also possible to obtain ΔC_p with good precision. To our knowledge, few studies reported in the literature take advantage of this technique to characterize the complexation between oligonucleotides (*43*−*48*), and only one reports data pertaining to the pairing of LNA/DNA strands to their complementary RNA strand (*36*).

With the aim to contribute to the understanding of the physicochemical principles underlying the remarkable properties of LNA, we used ITC to study the pairing thermodynamics of an 11 base-pair synthetic full-LNA:DNA duplex and of its

5′-CGCACACACGC-3′ DNA 5′-CGCACACACGC-3′ LNA
3′-GCGTGTGTGCG-5′ DNA 3′-GCGTGTGTGCG-5′ DNA

isosequential DNA:DNA duplex. The thermal stability of the twosystems was also monitored, for comparison reasons, by UV absorption spectroscopy and by DSC. The oligonucleotide was chosen as it has already been the subject of many structural studies. The natural duplex is known to form a full B-DNA type turn (*49*). Its sequence and length are furthermore particularly well adapted to physicochemical studies, including NMR studies (*49*, *50*).As LNA containing oligonucleotides have potential in various applications where base-pair opening is of utmost importance, we also investigated the effect of LNA on base-pair opening dynamics by comparing, via NMR experiments, the exchange times of the imino protons of the hybrid duplex with those of the natural duplex. Proton exchange studies have been reported for different DNA duplex conformations (*51*−*55*), drug−DNA complexes (*56*), tRNA (*57*) and RNA duplexes (*55*, *58*), but to our knowledge no data pertaining to the base-pair dynamics of LNA containing oligonucleotides have been reported in the literature.

MATERIALS AND METHODS

Preparation of Samples. The two DNA strands and the LNA strand were purchased in the sodium salt form from Eurogentec (Belgium). The cytosines in the LNA strand are all methylated (5-Me-C-LNA). All batches were dialyzed previous to any use against a large volume of milli-Q H_2O with a MW cutoff of 1 kDa. Pairing of the strands was achieved by heating a solution containing an equal number of moles of each strand to 95 °C for 10 min and then letting the system cool slowly. The obtained duplex was dialyzed against a large volume of milli-Q H_2O with a MW cutoff of 3.5 kDa and lyophilized before dilution in the desired buffer. The oligonucleotide concentrations were determined spectrophotometrically by measuring the absorbance at room temperature at 260 nm and using $\varepsilon = 99\,600\ M^{-1}\ cm^{-1}$ for the strand 5′-CGCACACACGC-3′ called strand A, $\varepsilon = 101\,300\ M^{-1}\ cm^{-1}$ for the strand 5′-GCGTGTGTGCG-3′ called strand T and $\varepsilon = 168\,200\ M^{-1}\ cm^{-1}$ for the duplexes. The ε value of the DNA:DNA duplex was previously determined in our laboratory (details given in ref *59*). The ε values for the single strands were obtained using the nearest neighbor model and its published parameters for DNA at room temperature (*60*). The coefficients used for the LNA single strand and the hybrid duplex were the same as those used for the homologous DNA systems. The change with temperature (between 5° and 60 °C) of the ε values of the single strands at 260 nm was less than 2%.

A pH = 7, 10 mM sodium phosphate buffer with 100 mM NaCl and 0.1 mM EDTA, was used for the thermal denaturation (UV, DSC, NMR), CD and ITC experiments.

UV Melting experiments were carried out with a Perkin-Elmer lambda-40 spectrophotometer equipped with a PTP-1 DNA melting kit. Absorbance vs temperature curves were measured using a heating rate of 1 K/min. The temperature was measured directly in the sample using a thermocouple adapted to the cell cap. The absorbance was measured, depending on sample concentration, at either 260 or 290 nm and using either a 10 mm or a 2 mm path length. Concentrations ranged between 1 μM and 100 μM for the duplexes and between 5 μM and 20 μM for the single strands. The T_m and $\Delta H°(T_m)$ were derived from the denaturation curves using the well described "two-state" model (*50*, *61*) where the absorbance is expressed as a function of α, the fraction of strands in the single strand form, A_{ds}, the absorbance of the solution containing only the duplex and A_{ss}, the absorbance of the solution containing only single strand oligonucleotides (eq 1):

$$A_{obs} = (1-\alpha)A_{ds} + \alpha A_{ss} \quad (1)$$

An expression for α can be extracted from eq 2 (where C_o is the total concentration of each strand) and inserted into eq 1 which can then be fitted to the experimental melting curve

treating $\Delta H°$, T_m, and the parameters describing the linear variation of A_{ds} and A_{ss} with temperature as variable parameters.

$$\frac{\alpha^2 C_0{}^2}{C_0(1-\alpha)} = \exp\left(-\frac{\Delta H^0}{R}\left(\frac{1}{T}-\frac{1}{T_m}\right)+\ln\frac{C_0}{2}\right) \quad (2)$$

At least five runs were performed for each sample and reported errors correspond to the 95% confidence interval.

DSC experiments were carried out using a scan rate of 1 K/min with a Calorimetric Science Corporation nanoDSC-II differential adiabatic scanning microcalorimeter equipped with 0.3268 mL cells. Integration of the area between the C_p versus T curve and the baseline, constructed using the two-state model, yields the transition enthalpy ($\Delta H°(T_m)$) and T_m is the temperature which divides this area in two. All data were processed using the standard CSC software. Concentrations ranged between 25 and 100 μM for the duplexes and experiments were run on the single strands at a concentration of approximately 200 μM. At least five runs were performed for each sample, and reported errors correspond to the 95% confidence interval.

ITC experiments were performed on an ITC-4200 from Calorimetric Science Corporation. Aliquots of 5 μL of a solution of one of the strands of a known precise concentration (in the 250 μM range) were injected into the 1.3 mL titration cell containing the solution of the complementary strand (in the 10 μM range). Twenty injections were typically performed for each set of experimental conditions at intervals of 600 s to ensure the return to equilibrium. Blank experiments were performed in order to take ligand dilution heat into consideration (heat removed before analyzing the titration data). Fitting of a 1:1 binding model to the experimental data was undertaken with program developed in-house, using a simplex algorithm to minimize a cost function which takes into account the errors on (i) the heat exchanges after each injection (at least three individual baselines were constructed in order to estimate an error on the individual Q_i) and on (ii) the concentrations in the cell (linked to errors on ε and on the volume of injection). The heat of the first injection was systematically removed for analysis.

CD spectra were recorded at room temperature for both duplexes at a concentration of 140 and 75 μM for the LNA:DNA and DNA:DNA duplexes, respectively, on a JASCO J-710 CD spectrometer with a 0.02 cm cell. Each CD spectrum was the accumulation of eight scans recorded at 50 nm/min with a 1 nm slit and a time constant of 0.5 s for a nominal resolution of 0.5 nm. Data were collected from 200 to 320 nm.

One dimensional ^1H NMR experiments were acquired, at different temperatures, on a Varian Unity - 600 MHz spectrometer using the jump-return pulse sequence with a delay which maximizes the imino proton intensities (50 μs) (*62*). Spectra were recorded with a minimum of 512 transients, an acquisition time of 2 s, a recycle delay of 2 s, a spectral width of 12000 Hz, and a digital resolution of at least 0.5 Hz/pt. The FIDs were weighted by a 2 Hz exponential multiplication prior to Fourier transformation. Concentrations of the single strands and of the duplexes were approximately 200 μM.

The assignment of the signals of the DNA:DNA duplex has been previously reported (*49*) and the assignment of the DNA:LNA imino protons was achieved by 2D NOESY spectra collected with mixing times ranging from 100 to 300 ms.

Imino proton exchange experiments were performed at 20 and 15 °C using NH_3 as proton acceptor. The formalism of catalyzed imino proton exchange is described in the literature (*63*). Imino protons exchange with water from the transiently open state via an acid−base reaction catalyzed by proton acceptors. The proton acceptor contribution to the exchange time is given by

$$\tau_{ex,cat} = \tau_{cl} + \frac{1+10^{pK(nu)-pK(acc)}}{\alpha k_{coll} K_d [acc]} \quad (3)$$

where τ_{cl} is the base-pair lifetime, K_d is the base-pair dissociation constant (τ_{op}/τ_{cl}), k_{coll} is the collision rate (considered here to be equal 10^9 s^{-1}) (*63*), pK(nu) is the pK of the monitored nucleotide imino proton (9.3 for G and 10.3 for T) (*54*), pK(acc) is the pK of the proton acceptor, (p$K(NH_3)$ = 9.3), [acc] is the proton acceptor concentration and α is the accessibility factor of the proton acceptor for the imino protons in the open state (considered equal to 1 when NH_3 is used as proton acceptor) (*63*). The exchange contribution of the catalyst, $\tau_{ex,cat}$, was determined from the exchange times measured in the presence (τ_{ex}) and in the absence ($\tau_{ex,0}$) of ammonia:

$$\tau_{ex,cat} = \left(\frac{1}{\tau_{ex}} - \frac{1}{\tau_{ex,0}}\right)^{-1} \quad (4)$$

The plot of $\tau_{ex,cat}$ versus the inverse of catalyst concentration yields τ_{cl} and the dissociation constant.

Samples of lyophilized duplex were dissolved at a concentration in the 500 μM range in a 90% H_2O/10% D_2O solution containing 1 mM EDTA. The pH was adjusted to 8.9 using concentrated solutions of NaOH and HCl. Aliquots of 6.5 M NH_4Cl were added to the initial solution to increase the catalyst concentration and the pH readjusted to 8.9 after each addition.

Exchange times were determined by magnetization transfer from water (*63*). Water magnetization was inverted using a DANTE sequence of six 30° hard pulses separated by 100 μs intervals. The residual transverse component was destroyed by a Z gradient (23 G/cm) applied after the DANTE sequence (500 μs) and a Z-gradient (0.01 G/cm) was also applied during the magnetization transfer delay (δ) to reduce radiation damping. The signal was detected using an echo water suppression subsequence with a 50 μs delay which maximizes the imino proton intensities (*64*). A 300 μs gradient was applied before recording the FID (15 G/cm). A recovery delay of 15 s was used in order to allow full relaxation of the water magnetization. The imino proton exchange times at different catalyst concentrations were obtained using a minimum of 23 time increments. The delay never exceeded 150 ms in order to avoid unwanted cross-relaxation effects. The longitudinal relaxation times of water ($R_{1,w}$) and of the imino protons ($R_{1,i}$) were determined with separate inversion−recovery experiments using a minimum of 11 time increments.

RESULTS AND DISCUSSION

Stability of the Duplexes. The thermal denaturation of the 11 base-pair DNA:DNA duplex was monitored by UV-spectroscopy and by DSC for duplex concentrations ranging between 1 μM and 100 μM. The T_m of the LNA:DNA duplex was too high, even at 1 μM, to be determined by UV-spectroscopy. It could however be estimated by DSC as it is possible to heat the sample to temperatures slightly above 100 °C in a DSC cell (pressurized at 3 atm). The T_m values obtained for the natural and hybrid duplexes at similar

Table 1: T_m Derived from UV and DSC Thermal Denaturation Experiments for Different Concentrations of the DNA:DNA and LNA:DNA Duplexes[a]

	T_m (°C)	
[db] (μM)	DNA:DNA	LNA:DNA
100	68 ± 1	102 ± 2
50	64 ± 2	99 ± 2
25	62 ± 1	97 ± 2
1	54 ± 1	

[a]For the DNA:DNA duplex the value correspond to the mean of the UV and DSC experiments while for LNA only DSC gave appropriate results.

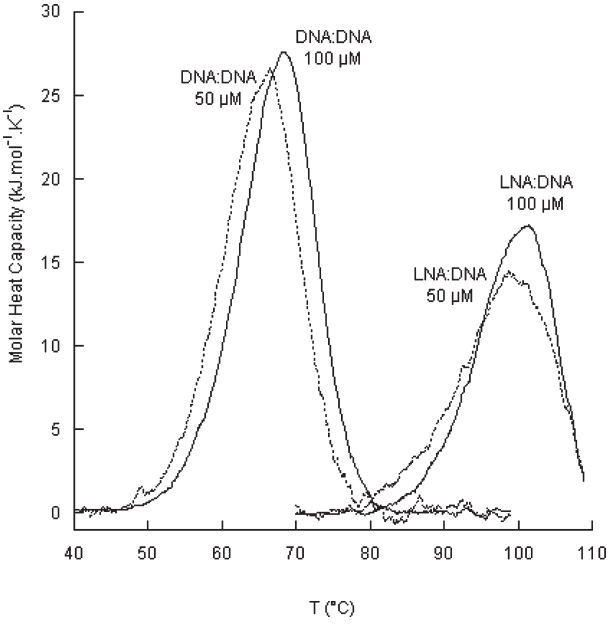

FIGURE 1: DSC thermograms (molar heat capacity) of the DNA:DNA and LNA:DNA duplexes at two different concentrations.

concentrations are reported in Table 1 and DSC thermograms are shown in Figure 1. The T_m of the LNA:DNA duplex are approximately 35 °C higher than those of the DNA:DNA duplex. These results are comparable to results reported in the literature for LNA:DNA duplexes studied under similar experimental conditions (*2*, *10*, *24*, *32*, *33*, *65*).

The thermodynamic parameters pertaining to the pairing of the strands of the DNA:DNA and LNA:DNA duplexes were obtained by isothermal titration calorimetry (ITC) at temperatures between 15 and 37 °C. Figure 2 shows ITC data acquired at 37 °C for the titration of DNA strand A or LNA strand A into the cell containing the DNA strand T (for all ITC results see Supporting Information). The heats of dilution of the single strands were taken into consideration when analyzing the data. They were found to be constant throughout the blank experiment and furthermore identical to the heat generated by the last injections in the pairing experiments. This indicates that there is no change in the aggregation states of the single strands. The parametric adjustment of the 1:1 binding model to the experimental data converges toward a larger value for the affinity constant for the LNA:DNA duplex, but as these K_a are very large and cannot be determined with precision, the data should only be considered qualitatively. Figure 3 shows the ITC determined $\Delta H°$ for both systems as a function of temperature. The $\Delta H°(T_m)$ of the DNA:DNA duplex extracted from the UV and DSC data are also shown for comparison. At all temperatures, $\Delta H°$ is less favorable for the formation of the LNA:DNA duplex than for that of the DNA:DNA duplex. As the LNA:DNA duplex is more stable than the DNA:DNA duplex, the entropic contribution ($T\Delta S°$) to duplex formation must consequently be less unfavorable for the LNA:DNA duplex.

The ^{1}H NMR spectra of the LNA single strand highlights that this strand adopts some structure at temperatures below 35 °C (see Supporting Information). Two imino proton signals are observed in the zone corresponding to the presence of H-bonds between correctly matched base-pairs. They are observed for high (200 μM) and low concentration (20 μM) solutions suggesting the presence of a monomolecular structure. The thermal monitoring of the LNA by UV highlights a melting transition with a T_m of 20 °C (concentrations between 5 and 20 μM) and characterized by a $\Delta H°(T_m)$ of -160 ± 40 kJ/mol (see Supporting Information). The denaturing of both DNA single strands did not exhibit a UV transition, and none of the strands exhibited a transition in the DSC scans.

The contribution of single strand order to the thermodynamics of duplex formation has been discussed in the literature (*44*, *48*, *66*, *67*) where it has clearly been shown that the initial state of the single strands can make an important contribution to the thermodynamic profile of duplex formation. The presence of structure in the LNA single strand will lead to a lower entropic penalty upon the formation of the hybrid duplex at lower temperatures, such as those monitored by ITC. This entropic gain will not be present at higher temperatures, such as those monitored by thermal denaturing experiments, as the single strand is no longer structured. The fact that the sugar moieties in the LNA single strand are blocked in a particular conformation will of course contribute, at all temperatures, to a difference in the $\Delta S°$ of interaction of the two duplexes.

As the structuring of the LNA single strand is not a favorable helical preorganization, the disruption of the intrastrand hydrogen bonds will contribute in an unfavorable way to enthalpy of formation of the hybrid duplex at lower temperatures. At temperatures close to the T_m of the LNA single strand (293 K), the $\Delta H°$ characterizing duplex formation is ~70 kJ/mol less favorable for the hybrid duplex compared to the natural one. If the $\Delta H°$ of the LNA single strand is taken into account (~160 kJ/mol), it is clear that at these temperatures, the enthalpy that characterizes the interaction between the two strands in the hybrid duplex is significantly more favorable than the one characterizing the interaction between the two DNA strands in the natural duplex. This clearly suggests that, as previously mentioned (*35*, *36*), enhanced stacking interactions exist in LNA containing duplexes due to their more A-type helical structure. CD spectra of the DNA:DNA and LNA:DNA duplex clearly highlight that the former adopts a B-type helical structure (one positive (~280 nm) and two negative, (~250 and ~210 nm) peaks of approximately same intensity), while the latter adopts a RNA A-type helical structure (a maximum around 260 nm, a small negative peak around 240 nm, an intense negative peak around 210 nm and a slightly negative CD between 280 and 310 nm) (*68*). It is also possible that the methyl groups present on the LNA cytosines lead to more favorable London interaction in the hybrid duplex (*69*).

Analysis of the ITC data clearly shows that the $\Delta H°$ of both duplexes are temperature dependent. The slopes of the linear regressions performed on the ITC data (lines shown in Figure 3)

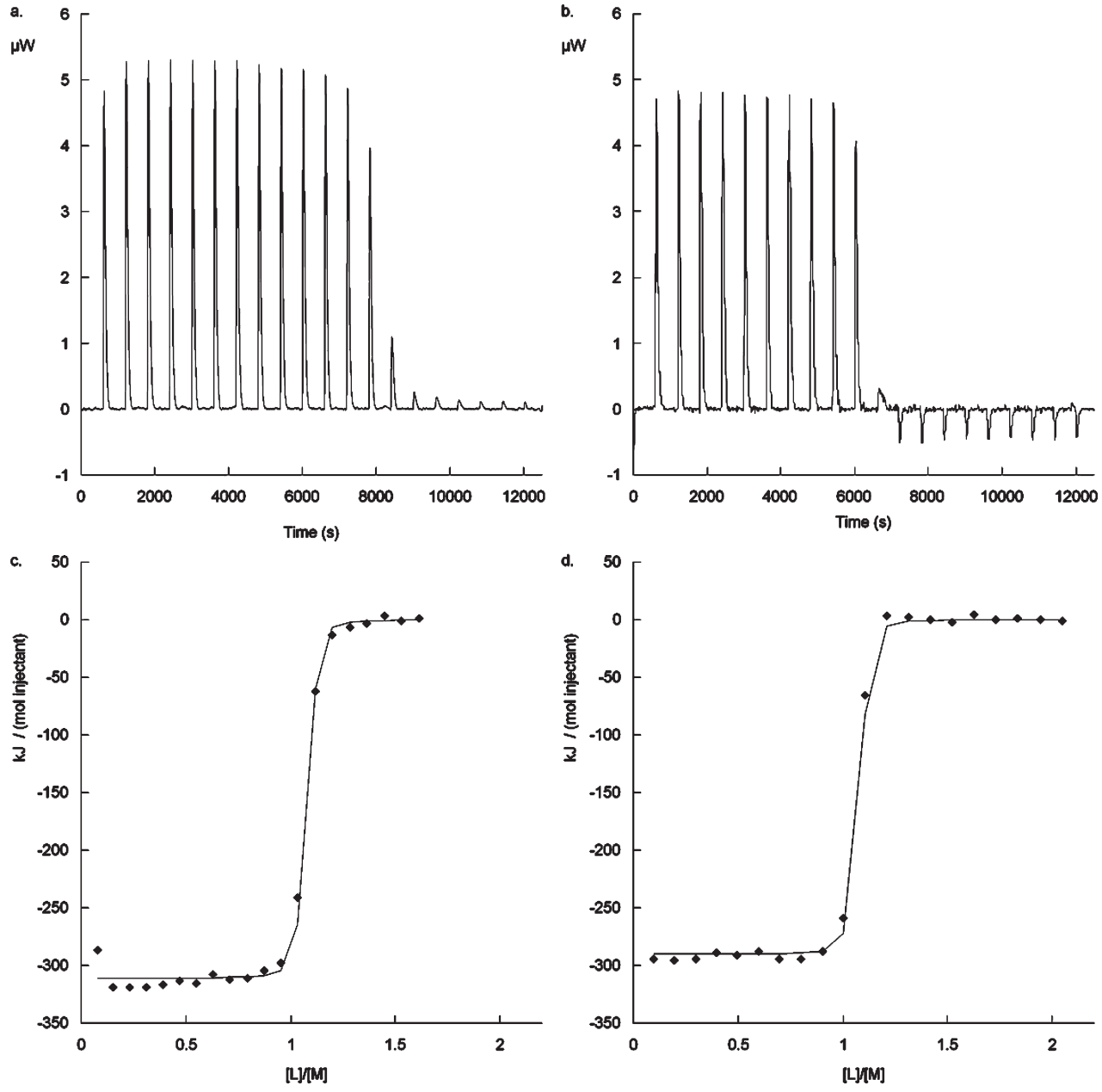

FIGURE 2: ITC titration profiles (upper panels) at 37 °C and enthalpies (lower panels) for the formation of the (A) DNA:DNA duplex and (B) LNA:DNA duplex. Blank experiments were run for all experiments to remove heats of dilution. The solid lines in the lower panels correspond to a 1:1 binding fit. The first data point was omitted from the fitting procedure. Concentration of DNA strand T in the cell was 10 μM for both titrations and the concentrations of ligand in the syringe were 200 and 230 μM for the DNA and LNA experiments, respectively.

yield ΔC_p values of -3.7 ± 0.3 kJ mol^{-1} K^{-1} and -6.3 ± 0.6 kJ mol^{-1} K^{-1} for the DNA:DNA and LNA:DNA duplexes, respectively. These values are obtained with a much greater accuracy and precision than the ones that can be derived from thermal denaturation studies. It is indeed impossible to estimate a ΔC_p with good precision from the concentration dependence of the $\Delta H°(T_m)$ determined by UV and DSC, not only because the temperature range is usually extremely narrow but also because of the scatter and large experimental errors associated with $\Delta H°$ values derived from denaturation curves. Regarding the possibility of determining $\Delta C_p(T_m)$ by measuring the difference, at T_m, between the pre- and post-transitional baselines of a DSC thermogram, it is known that ΔC_p determined in this way are highly dependent on the choice of baselines – small perturbations in the regions assigned to the baseline can produce large changes in the ΔC_p (*41*–*43*).

No data on ΔC_p of LNA containing oligonucleotides have to our knowledge been reported in the literature. ITC derived values for various long DNA and RNA polynucleotides seem to indicate that their ΔC_p are essentially independent of sequence and of the nature of the nucleotide (DNA or RNA). An average value of 268 ± 33 J mol^{-1} K^{-1} per base-pair has been reported (*41*). The ITC determined ΔC_p reported for shorter systems exhibit some variation with sequence and length (*45*–*48*, *70*) with values for DNA:DNA and RNA:DNA duplexes, ranging between −1.42 kJ mol^{-1} K^{-1} (*47*) and −5.43 kJ mol^{-1} K^{-1} (*48*). Differences are observed in the ΔC_p of homologous DNA:DNA and RNA:DNA duplexes but with no systematic deviation (*47*, *70*). The value determined in this study for the DNA:DNA duplex falls in the range of the ones reported in the literature for duplexes of similar length, while the value determined for the LNA:DNA duplex is somewhat higher.

An explanation for the molecular origin of the large negative ΔC_p of duplex formation is temperature-dependent changes in the thermodynamic state of the single strands (*42*, *43*, *46*, *48*). The larger ΔC_p observed for the LNA:DNA duplex is most certainly the consequence of the fact that the LNA single strand adopts some structure at temperatures below 35 °C. In the higher temperature range sampled by thermal scanning methods, single strands are always essentially random coil and the ΔC_p measured via these methods will consequently not be influenced by an eventual coupled temperature-dependent equilibrium related to the single strands. The line drawn through the ITC determined $\Delta H°$ values reported in Figure 3 and whose slope yields the ΔC_p value can consequently not be extrapolated to higher temperatures. It can be expected that at higher temperatures the difference in the ΔC_p of the hybrid and natural duplex will essentially disappear.

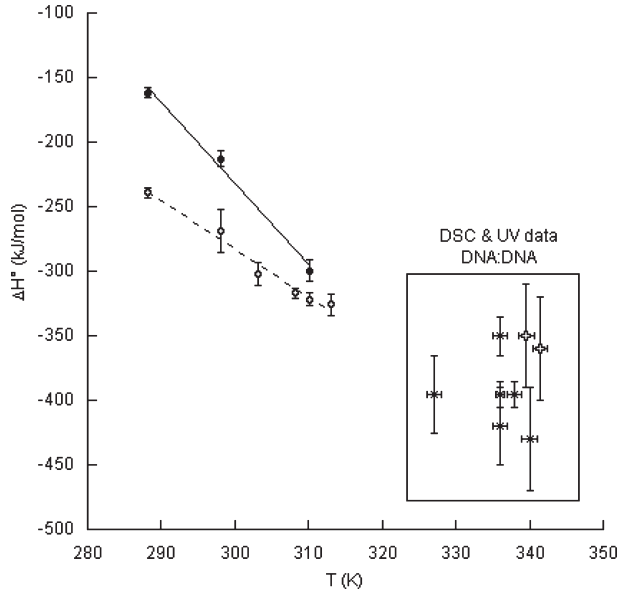

FIGURE 3: Enthalpies of formation ($\Delta H°$) for the DNA:DNA (open circles) and the LNA:DNA (filled circles) duplexes as a function of temperature. The data obtained by UV and DSC are highlighted. The lines represent the linear weighted least-squares fits to the DNA:DNA (dashed line) and LNA:DNA (solid line) ITC data. The derived ΔC_p are 3.7 ± 0.3 kJ mol^{-1} K^{-1} and 6.3 ± 0.6 kJ mol^{-1} K^{-1} for the DNA:DNA and LNA:DNA duplexes, respectively.

Base-Pair Opening Dynamics. The imino proton region in the ^{1}H NMR spectra of the DNA:DNA and LNA:DNA duplexes are shown in Figure 4 as a function of temperature with assignments indicated in the lowest temperature spectra. The signal intensities of the imino protons of both duplexes decrease with temperature as a consequence of their exchange with water protons. Exchange takes place when the hydrogen bond in which the imino proton is implicated is broken and when the lifetime of the open state is sufficient for proton transfer to occur (*51*). The exchange process, characterized by the rate constant k_{ex}, is consequently a function of the base-pair lifetime (τ_{cl}), the lifetime of the open state (τ_{op}), and the rate of transfer of the imino proton from the nucleoside to the proton acceptor (k_{tr}). These lifetimes and rate constants are temperature dependent and are furthermore different for each imino proton which explains why the different signals in the ^{1}H spectrum do not all disappear at the same temperature (*51*, *71*−*73*).

In both duplexes the first signals to disappear are those which correspond to the terminal guanines (G12 and G22) and the signals of the guanines next to the terminal ones (G2 and G10) are the next to disappear. These data clearly indicate that fraying of the two last base-pairs occurs in both systems. The signals of all other imino protons disappear between 60 and 70 °C in the homoduplex, but not all have disappeared at 85 °C in the heteroduplex. As the LNA:DNA duplex exhibits the higher T_m, this is not surprising. It is however difficult to try and relate these disappearance temperatures to the T_m, which characterizes the duplex as a whole and not at the individual base-pair level.

The imino proton exchange process at the level of an individual base-pair can be described using a two-state (open/closed) model where the imino protons are protected within the closed pair but can exchange from the transiently open pair, via an acid−base reaction catalyzed by proton acceptors (*63*). The formalism of catalyzed imino proton exchange from a base-pair has been extensively described in the literature and the two state model validated (*54*, *63*). The base-pair lifetime (τ_{cl}) is equal to the imino proton exchange time if exchange occurs at each opening event, that is, in the presence of high proton acceptor concentrations.

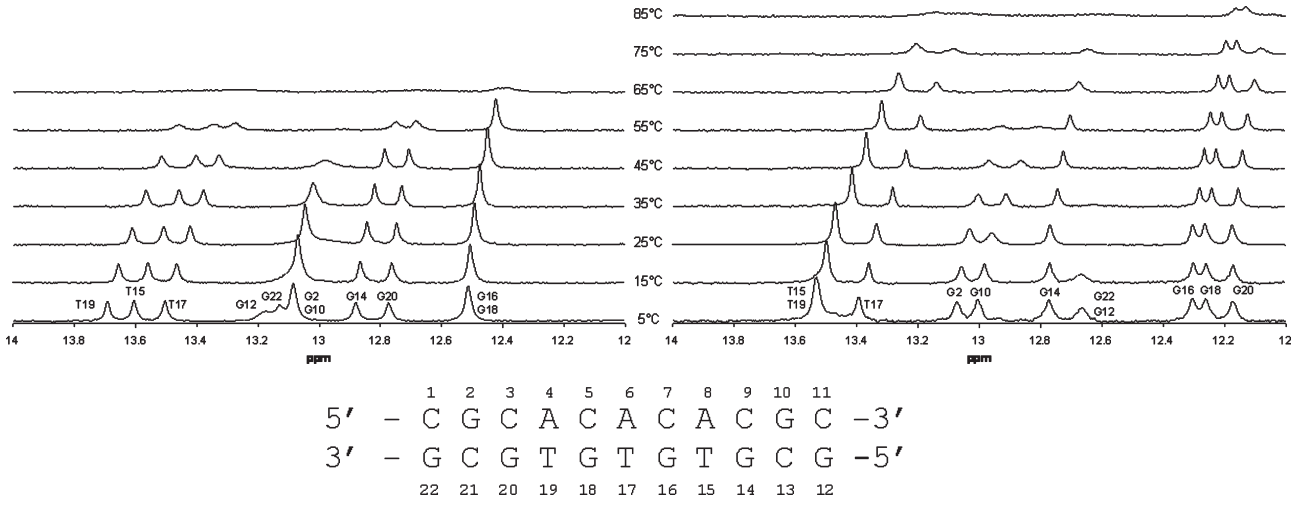

FIGURE 4: Imino signals of the (a) DNA:DNA and (b) LNA:DNA duplexes as a function of temperature. Peaks assignments are indicated on the spectra recorded at 5 °C.

When the proton acceptor concentration is limiting, the imino proton transfer rate is function of the apparent base-pair dissociation constant, K_d, which is the ratio of the lifetimes of the open and closed states of the base-pair (τ_{op}/τ_{cl}). The plot of the proton acceptor contribution to the imino proton exchange time, $\tau_{ex,cat}$, versus the inverse of the acceptor concentration is, according to the model, a straight line whose extrapolation to infinite catalyst concentration yields the base-pair lifetime; K_d can be derived from the slope (see the Materials and Methods section) (*51*, *58*, *63*).

In order to extract information on the opening dynamics of a base-pair, it is necessary to integrate the signal of the imino proton which is involved in the hydrogen bond between the two complementary bases. The imino signals which are well resolved in both the DNA:DNA and in the LNA:DNA duplex are the signals of T17, G14, and G20, and these three imino protons were monitored in both systems at 15 and 25 °C. Figure 5 shows the imino proton region at 25 °C of both duplexes in the absence and in the presence of 10 mM of the proton acceptor, NH_3. The signals broaden considerably as the catalyst concentration increases.

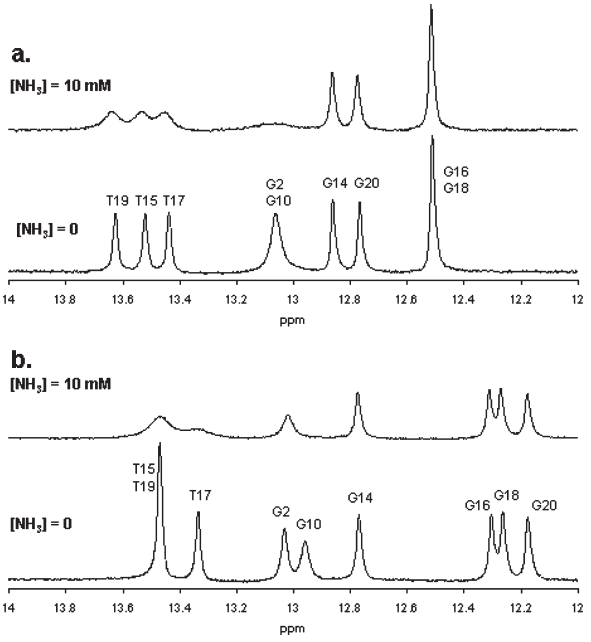

FIGURE 5: Imino signals of the (a) DNA:DNA and (b) LNA:DNA duplexes at 25 °C in the absence (lower spectra) and in the presence of approximately 10 mM NH_3 (upper spectra).

The proton acceptor contribution, $\tau_{ex,cat}$, to the imino exchange times are shown in Figure 6 as a function of the inverse of the proton acceptor concentration. The data were fitted with a least-squares parametric adjustment to a straight line (see eq 1). The τ_{cl} and K_d obtained for each base are given in Table 2. The T17 imino signal broadens in both systems very quickly upon catalyst addition and τ_{cl} could consequently not be obtained with acceptable precision. The $\tau_{ex,cat}$ determined for the highest catalyst concentration is considered as an upper limit, but not as a good estimate, for τ_{cl}.

Even if the τ_{cl} of the A-T pair could not be obtained with good precision, it is clear from the comparison of the $\tau_{ex,cat}$ values (Figure 6) that in both systems the lifetime of the A-T pair is smaller than those of the G-C pairs, which is not surprising considering the more extensive hydrogen bonding of G-C base-pairs. It has been reported that in DNA:DNA duplexes, G-C base-pair lifetimes range between 5 and 50 ms and that those of A-T base-pairs range between 0.5 to 7 ms (*74*). The τ_{cl} of the two G-C pairs in the DNA:DNA duplex fall in the upper range of those reported in the literature and are smaller at 25 °C than at 15 °C. The τ_{cl} of the two G-C pairs in the LNA:DNA hybrid duplex are larger than those of the corresponding pair in the DNA:DNA duplex and are only slightly affected by the change in temperature.

Table 2: Base-Pair Dissociation Constant, K_d, and Base-Pair Lifetime, τ_{cl}, of the G20, G14, and T17 Imino Protons in the DNA:DNA and LNA:DNA Duplexes at 25 °C and 15 °C

	G20		G14		T17	
	K_d (10^{-6})	τ_{cl} (ms)	K_d (10^{-6})	τ_{cl} (ms)	K_d (10^{-6})	τ_{cl} (ms)[a]
DNA:DNA						
25 °C	2.42 ± 0.15	7 ± 9	2.13 ± 0.02	15 ± 12	91 ± 11	(< 27)
15 °C	0.63 ± 0.02	41 ± 12	0.61 ± 0.02	71 ± 16	35 ± 3	(< 14)
LNA:DNA						
25 °C	0.68 ± 0.03	35 ± 25	0.65 ± 0.05	70 ± 34	185 ± 21	(< 8)
15 °C	0.32 ± 0.15	31 ± 27	0.79 ± 0.15	83 ± 24	31 ± 3	(< 4)

[a]For the T17 base-pair, τ_{cl} could not be obtained from the adjustment of eq 1 to the experimental data points and the upper limit of τ_{cl} which is indicated corresponds to the $\tau_{ex,cat}$ at the highest concentration in catalyst for which the signal could still be integrated.

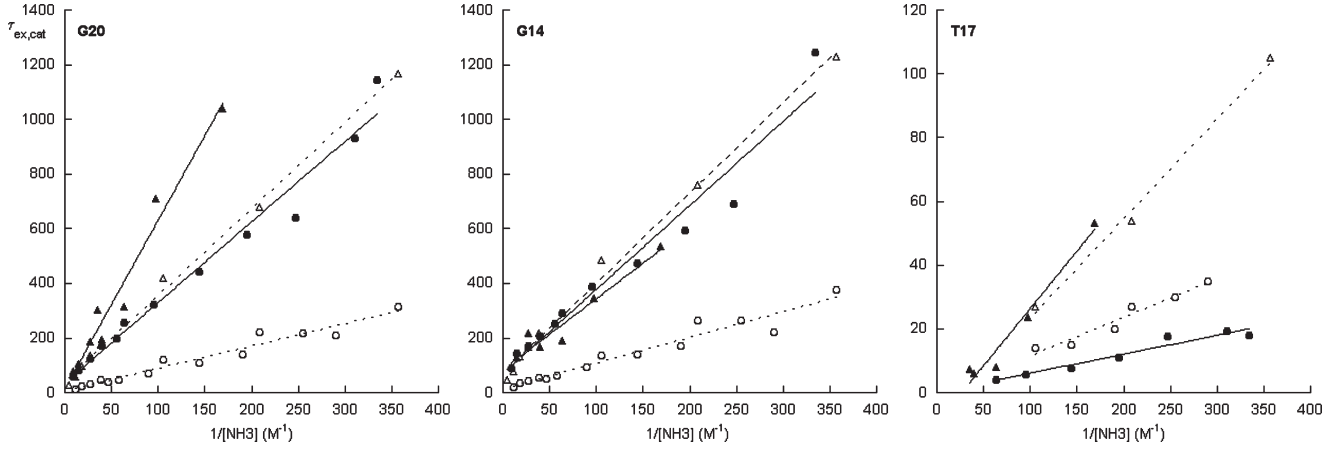

FIGURE 6: Proton acceptor contribution at 25 °C (circles) and 15 °C (triangles) for the (a) G20, (b) G14, and (c) T17 imino exchange times as a function of the inverse of the proton acceptor concentration. Filled symbols and full lines relate to the LNA:DNA duplex and open symbols and dashed lines relate to the DNA:DNA duplex. Lines correspond to a least-squares linear adjustment of eq 3 to the experimental data points.

Base-pair lifetimes, like all kinetic parameters, do not directly provide structural information but are sensitive to local structure. The study of a series of homologous RNA and DNA duplexes (*54*) highlights that the lifetimes of r(G-C) pairs in the A-type helices tend to be longer than those of the equivalent d(G-C) pairs in the B-type helices. The values obtained in this study highlight that similar structural considerations could be valid as the G-C base-pairs have a longer lifetime at 25 °C in the A-type hybrid duplex. At 15 °C, considering the large uncertainties on these values, it is unfortunately difficult to conclude anything.

Regarding the dissociation constants, the K_d of the A-T base-pair is, in both systems and at both temperatures, more than an order of magnitude larger than the K_d of the G-C base-pairs. This is consistent with data reported in the literature which highlights that the G-C dissociation constants in DNA:DNA duplexes are on the order of 10^{-6} and while those of A-T base-pairs are at least 1 order of magnitude larger (*58*). The substitution of cytosine DNA nucleotides by their corresponding LNA equivalent increases the stability (in other words, decreases K_d) of both the C9-G14 and C3-G20 base-pairs at 25 °C. The effect is less pronounced at 15 °C which is a consequence of the weaker temperature dependence of the K_d values of the more stable LNA:DNA pairs than of the DNA:DNA pairs. Values obtained for the K_d of the C7-G16 ($0.28 \pm 0.02\ 10^{-6}$ at 15 °C and $0.38 \pm 0.02\ 10^{-6}$ at 25 °C) and C5-G18 ($0.29 \pm 0.02\ 10^{-6}$ at 15 °C and $0.35 \pm 0.02\ 10^{-6}$ at 25 °C) base-pairs in the hybrid duplex display the same relatively weak influence of temperature. They present a slightly higher stability compared to the C9-G14 and C3-G20 base-pairs which could be due to their more central position in the sequence. Unfortunately, no comparisons can be made with the equivalent protons in the DNA:DNA duplex as their NMR signals are not resolved . Concerning the K_d of the A6-T17 base-pair, the substitution of the adenine DNA nucleotide by its LNA equivalent has almost no effect on the dissociation constant at 15 °C and a destabilizing one at 25 °C. In this case, the temperature has a strong influence on K_d in both systems.

The study of the base-pair opening dynamics of homologous RNA and DNA duplexes (*54*) has shown that *r*(G-C) dissociation constants are smaller than *d*(G-C) dissociations constants while *r*(A-U) and *d*(A-T) pairs exhibit comparable stabilities. These results also highlight that structural features strongly influence base-pair dynamics. The K_d values obtained at 15 °C for the LNA:DNA duplex are similar to the values obtained for RNA duplexes. Our results are furthermore coherent with the results reported by McTigue et al.(*34*), who studied the effect of the incorporation of a single LNA nucleotide on the stability of a DNA duplex, and confirmed by those of You et al. (*75*). They conclude that, even if there is an important nearest neighbor dependence for each LNA base, LNA pyrimidines contribute more to stability than purines. The largest stabilizing effect is observed for the incorporation of a LNA cytosine and the smallest for an adenine, which is also observed in this study at the level of individual base-pairs. Base-pairs lifetimes have been correlated to the difficulty of breaking Watson−Crick hydrogen bonds and local stacking interactions (*76*). The increased lifetime for G-C base-pairs in LNA:DNA heteroduplex correlates well with the thermodynamic data reported for the LNA:DNA duplex.

In Summary. We have monitored the stability and base-pair dynamics of two isosequential duplexes, one composed of two DNA strands the other of a full-LNA and a DNA strand. As well documented in the literature, the substitution of DNA nucleotides by LNA nucleotides increases the thermal stability of the duplex and induces an A-type helical conformation. Using ITC we were able to highlight that the entropic term of duplex formation is less unfavorable for the heteroduplex than for the homoduplex. The locking of the sugar in the LNA nucleotides of course contributes to this $\Delta\Delta S°$, but the presence of a hairpin structure in the LNA single strand, highlighted by NMR and UV measurements, is also favorable from this point of view. The presence of this structure has however an unfavorable effect on the enthalpy of duplex formation as intrastrand H-bonds must be broken upon duplex formation. Taking this contribution into consideration, it is possible to show that the enthalpy of formation of the heteroduplex from unstructured single strands would be more favorable than the enthalpy of formation of the homoduplex. This suggests a more efficient stacking of the bases in the LNA containing duplex. The single strand structure will also partially explain the large ΔC_p associated with the formation of the hybrid duplex.

The determination by NMR magnetization transfer experiments of individual base-pair dissociation constants provides complementary information pertaining to the stability of the duplexes at the level of the individual base-pairs. The substitution of a cytosine by its LNA equivalent decreases the dissociation constant of the G-C base-pair and increases its lifetime, while an LNA substitution in an A-T base-pair does not seem to have a favorable effect on its stability. A decrease in temperature does not have an as important effect on the stability of a C-G base-pair in the LNA:DNA duplex than in the DNA:DNA duplex. This could be related to the fact that LNA nucleotides have less conformational freedom, making them less sensitive to a change in temperature. A more complete picture of base-pair dynamics of LNA containing oligonucleotides could be helpful in the design of displacement probes and primers used in hybridization-based assay, where it is likely that polymerase activity is dependent on the base-pair opening dynamics. The results of the base-pair dynamic experiments confirm the hypothesis, reflected by the more favorable $\Delta H°$ for the formation of the LNA:DNA duplex from unstructured strands, that noncovalent interactions in the LNA:DNA heteroduplex are more favorable than in the DNA:DNA homoduplex.

Our conclusions are based on the comparison of the results obtained for two isosequential duplexes (DNA:DNA and a full-LNA:DNA) and comparison with other sequences and/or with nucleotides with selective LNA substitutions would be needed in order to obtain more general conclusions regarding the effect of the incorporation of LNA nucleotides on the dynamics, thermodynamics, and thermal stability of oligonucleotides. Even if much work is still needed to elucidate all the factors at the origin of the increase in thermodynamic and thermal stability of a duplex induced by LNA substitutions, it is clear that the combined use of different experimental tools (ITC, NMR, thermal denaturation methods) helps to obtain a more complete picture at the molecular level.

ACKNOWLEDGMENT

The authors thank Prof. Michel Luhmer for helpful discussions pertaining to the NMR experiments and Dr. Vincent Raussens for help with the CD measurements.

SUPPORTING INFORMATION AVAILABLE

^{1}H NMR spectra of the imino region of the LNA single strand as a function of temperature and concentration. Thermal dena-

turation curve of the LNA single strand monitored by UV absorption spectroscopy. A table summarizing the enthalpies of formation ($\Delta H°$) determined at different temperatures by ITC for the DNA:DNA and LNA:DNA duplexes.This material is available free of charge via the Internet at http://pubs.acs.org.

REFERENCES

1. Singh, S. K., Nielsen, P., Koshkin, A. A., and Wengel, J. (1998) LNA (locked nucleic acids): synthesis and high-affinity nucleic acid recognition. *Chem. Commun.* 455–456.
2. Koshkin, A. A., Nielsen, P., Meldgaard, M., Rajwanshi, V. K., Singh, S. K., and Wengel, J. (1998) LNA (locked nucleic acid): an RNA mimic forming exceedingly stable LNA:LNA duplexes. *J. Am. Chem. Soc. 120*, 13252–13253.
3. Egli, M., Teplova, M., Minasov, G., Kumar, R., and Wengel, J. (2001) X-ray crystal structure of a locked nucleic acid (LNA) duplex composed of a palindromic 10-mer DNA strand containing one LNA thymine monomer. *Chem. Commun.* 651–652.
4. Petersen, M., and Wengel, J. (2003) LNA: a versatile tool for therapeutics and genomics. *Trends Biotechnol. 21*, 74–81.
5. Vester, B., and Wengel, J. (2004) LNA (locked nucleic acid): high-affinity targeting of complementary RNA and DNA. *Biochemistry 43*, 13233–13241.
6. Jepsen, J. S., Sorensen, M. D., and Wengel, J. (2004) Locked nucleic acid: A potent nucleic acid analog in therapeutics and biotechnology. *Oligonucleotides 14*, 130–146.
7. Kaur, H., Babu, B. R., and Maiti, S. (2007) Perspectives on chemistry and therapeutic applications of locked nucleic acid (LNA). *Chem. Rev. 107*, 4672–4697.
8. Elmen, J., Thonberg, H., Ljungberg, K., Frieden, M., Westergaard, M., Xu, Y., Wahren, B., Liang, Z., Urum, H., Koch, T., and Wahlestedt, C. (2005) Locked nucleic acid (LNA) mediated improvements in siRNA stability and functionality. *Nucleic Acids Res. 33*, 439–447.
9. Fluiter, K., Mook, O. R. F., and Baas, F. (2009) The therapeutic potential of LNA-modified siRNAs: reduction of off-target effects by chemical modification of the siRNA sequence. *Methods Mol. Biol. 487*, 189–203.
10. Wahlestedt, C., Salmi, P., Good, L., Kela, J., Johnsson, T., Hokfelt, T., Broberger, C., Porreca, F., Lai, J., Ren, K., Ossipov, M., Koshkin, A., Jakobsen, N., Skouv, J., Oerum, H., Jacobsen, M. H., and Wengel, J. (2000) Potent and nontoxic antisense oligonucleotides containing locked nucleic acids. *Proc. Natl. Acad. Sci. U. S. A. 97*, 5633–5638.
11. Arzumanov, A., Walsh, A. P., Rajwanshi, V. K., Kumar, R., Wengel, J., and Gait, M. J. (2001) Inhibition of HIV-1 Tat-dependent trans activation by steric block chimeric 2′-O-methyl/LNA oligoribonucleotides. *Biochemistry 40*, 14645–14654.
12. Elayadi, A. N., Braasch, D. A., and Corey, D. R. (2002) Implications of high-affinity hybridization by locked nucleic acid oligomers for inhibition of human telomerase. *Biochemistry 41*, 9973–9981.
13. Ruiz-Ruiz, S., Moreno, P., Guerri, J., and Ambros, S. (2009) Discrimination between mild and severe Citrus tristeza virus isolates with a rapid and highly specific real-time reverse transcription-polymerase chain reaction method using TaqMan LNA probes. *Phytopathology 99*, 307–315.
14. Stenvang, J., Lindow, M., and Kauppinen, S. (2008) Targeting of microRNAs for therapeutics. *Biochem. Soc. Trans. 36*, 1197–1200.
15. Beane, R., Gabillet, S., Montaillier, C., Arar, K., and Corey, D. R. (2008) Recognition of chromosomal DNA inside cells by locked nucleic acids. *Biochemistry 47*, 13147–13149.
16. Veedu, R. N., Vester, B., and Wengel, J. (2008) Polymerase chain reaction and transcription using locked nucleic acid nucleotide triphosphates. *J. Am. Chem. Soc. 130*, 8124–8125.
17. Yamada, K., Terahara, T., Kurata, S., Yokomaku, T., Tsuneda, S., and Harayama, S. (2008) Retrieval of entire genes from environmental DNA by inverse PCR with pre-amplification of target genes using primers containing locked nucleic acids. *Environ. Microbiol. 10*, 978–987.
18. Ballantyne, K. N., van Oorschot, R. A. H., and Mitchell, R. J. (2008) Locked nucleic acids in PCR primers increase sensitivity and performance. *Genomics 91*, 301–305.
19. Gustafson, K. S. (2008) Locked nucleic acids can enhance the analytical performance of quantitative methylation-specific polymerase chain reaction. *J. Mol. Diagn. 10*, 33–42.
20. Kurreck, J., Wyszko, E., Gillen, C., and Erdmann, V. A. (2002) Design of antisense oligonucleotides stabilized by locked nucleic acids. *Nucleic Acids Res. 30*, 1911–1918.
21. Petersen, M., Nielsen, C. B., Nielsen, K. E., Jensen, G. A., Bondensgaard, K., Singh, S. K., Rajwanshi, V. K., Koshkin, A. A., Dahl, B. M., Wengel, J., and Jacobsen, J. P. (2000) The conformations of locked nucleic acids (LNA). *J. Mol. Recognit. 13*, 44–53.
22. Petersen, M., Bondensgaard, K., Wengel, J., and Jacobsen, J. P. (2002) Locked nucleic acid (LNA) recognition of RNA: NMR solution structures of LNA:RNA hybrids. *J. Am. Chem. Soc. 124*, 5974–5982.
23. Nielsen, K. E., Singh, S. K., Wengel, J., and Jacobsen, J. P. (2000) Solution structure of an LNA hybridized to DNA: NMR study of the d(CTLGCTLTLCTLGC):d(GCAGAAGCAG) duplex containing four locked nucleotides. *Bioconjug. Chem. 11*, 228–238.
24. Nielsen, K. E., Rasmussen, J., Kumar, R., Wengel, J., Jacobsen, J. P., and Petersen, M. (2004) NMR studies of fully modified locked nucleic acid (LNA) hybrids: solution structure of an LNA:RNA hybrid and characterization of an LNA:DNA hybrid. *Bioconjug. Chem. 15*, 449–457.
25. Nielsen, C. B., Singh, S. K., Wengel, J., and Jacobsen, J. P. (1999) The solution structure of a locked nucleic acid (LNA) hybridized to DNA. *J. Biomol. Struct. Dyn. 17*, 175–191.
26. Bondensgaard, K., Petersen, M., Singh, S. K., Rajwanshi, V. K., Kumar, R., Wengel, J., and Jacobsen, J. P. (2000) Structural studies of LNA:RNA duplexes by NMR: conformations and implications for RNase H activity. *Chem.- Eur. J. 6*, 2687–2695.
27. Ivanova, A., and Roesch, N. (2007) The structure of LNA:DNA hybrids from molecular dynamics simulations: the effect of locked nucleotides. *J. Phys. Chem. A 111*, 9307–9319.
28. Pande, V., and Nilsson, L. (2008) Insights into structure, dynamics and hydration of locked nucleic acid (LNA) strand-based duplexes from molecular dynamics simulations. *Nucleic Acids Res. 36*, 1508–1516.
29. Obika, S., Nanbu, D., Hari, Y., Andoh, J.-I., Morio, K.-I., Doi, T., and Imanishi, T. (1998) Stability and structural features of the duplexes containing nucleoside analogs with a fixed N-type conformation, 2′-O,4′-C-methyleneribonucleosides. *Tetrahedron Lett. 39*, 5401–5404.
30. Koshkin, A. A., Singh, S. K., Nielsen, P., Rajwanshi, V. K., Kumar, R., Meldgaard, M., Olsen, C. E., and Wengel, J. (1998) LNA (locked nucleic acids): synthesis of the adenine, cytosine, guanine, 5-methylcytosine, thymine and uracil bicyclonucleoside monomers, oligomerization, and unprecedented nucleic acid recognition. *Tetrahedron 54*, 3607–3630.
31. Singh, S. K., and Wengel, J. (1998) Universality of LNA-mediated high-affinity nucleic acid recognition. *Chem. Commun.* 1247–1248.
32. Orum, H., Jakobsen, M. H., Koch, T., Vuust, J., and Borre, M. B. (1999) Detection of the factor V Leiden mutation by direct allele-specific hybridization of PCR amplicons to photoimmobilized locked nucleic acids. *Clin. Chem. 45*, 1898–1905.
33. Braasch, D. A., and Corey, D. R. (2001) Locked nucleic acid (LNA): fine-tuning the recognition of DNA and RNA. *Chem. Biol. 8*, 1–7.
34. McTigue, P. M., Peterson, R. J., and Kahn, J. D. (2004) Sequence-dependent thermodynamic parameters for locked nucleic acid (LNA)-DNA duplex formation. *Biochemistry 43*, 5388–5405.
35. Kaur, H., Arora, A., Wengel, J., and Maiti, S. (2006) Thermodynamic, counterion, and hydration effects for the incorporation of locked nucleic acid nucleotides into DNA duplexes. *Biochemistry 45*, 7347–7355.
36. Kaur, H., Wengel, J., and Maiti, S. (2008) Thermodynamics of DNA-RNA heteroduplex formation: effects of locked nucleic acid nucleotides incorporated into the DNA strand. *Biochemistry 47*, 1218–1227.
37. Christensen, U., Jacobsen, N., Rajwanshi, V. K., Wengel, J., and Koch, T. (2001) Stopped-flow kinetics of locked nucleic acid (LNA)-oligonucleotide duplex formation: studies of LNA-DNA and DNA-DNA interactions. *Biochem. J. 354*, 481–484.
38. Christensen, U. (2007) Thermodynamic and kinetic characterization of duplex formation between 2′-O, 4′-C-methylene-modified oligoribonucleotides, DNA and RNA. *Biosci. Rep. 27*, 327–333.
39. Kierzek, E., Pasternak, A., Pasternak, K., Gdaniec, Z., Yildirim, I., Turner, D. H., and Kierzek, R. (2009) Contributions of stacking, preorganization, and hydrogen bonding to the thermodynamic stability of duplexes between RNA and 2′-O-methyl RNA with locked nucleic acids. *Biochemistry 48*, 4377–4387.
40. Kierzek, E., Ciesielska, A., Pasternak, K., Mathews, D. H., Turner, D. H., and Kierzek, R. (2005) The influence of locked nucleic acid residues on the thermodynamic properties of 2′-O-methyl RNA/RNA heteroduplexes. *Nucleic Acids Res. 33*, 5082–5093.
41. Tikhomirova, A., Taulier, N., and Chalikian, T. V. (2004) Energetics of nucleic acid stability: the effect of ΔCP. *J. Am. Chem. Soc. 126*, 16387–16394.

42. Mikulecky, P. J., and Feig, A. L. (2006) Heat capacity changes associated with nucleic acid folding. *Biopolymers 82*, 38–58.
43. Feig, A. L. (2007) Applications of isothermal titration calorimetry in RNA biochemistry and biophysics. *Biopolymers 87*, 293–301.
44. Jelesarov, I., Crane-Robinson, C., and Privalov, P. L. (1999) The energetics of HMG box interactions with DNA: thermodynamic description of the target DNA duplexes. *J. Mol. Biol. 294*, 981–995.
45. Takach, J. C., Mikulecky, P. J., and Feig, A. L. (2004) Salt-dependent heat capacity changes for RNA duplex formation. *J. Am. Chem. Soc. 126*, 6530–6531.
46. Mikulecky, P. J., and Feig, A. L. (2006) Heat capacity changes associated with DNA duplex formation: salt- and sequence-dependent effects. *Biochemistry 45*, 604–616.
47. Lang, B. E., and Schwarz, F. P. (2007) Thermodynamic dependence of DNA/DNA and DNA/RNA hybridization reactions on temperature and ionic strength. *Biophys. Chem. 131*, 96–104.
48. Holbrook, J. A., Capp, M. W., Saecker, R. M., and Record, M. T. Jr. (1999) Enthalpy and heat capacity changes for formation of an oligomeric DNA duplex: interpretation in terms of coupled processes of formation and association of single-stranded helices. *Biochemistry 38*, 8409–8422.
49. Jourdan, M. (1998) Ph.D. Thesis, Université Joseph Fourier, Grenoble, France.
50. Cahen, P., Luhmer, M., Fontaine, C., Morat, C., Reisse, J., and Bartik, K. (2000) Study by ^{23}Na-NMR, ^{1}H-NMR, and ultraviolet spectroscopy of the thermal stability of an 11-basepair oligonucleotide. *Biophys. J. 78*, 1059–1069.
51. Leroy, J. L., Kochoyan, M., Huynh Dinh, T., and Gueron, M. (1988) Characterization of base-pair opening in deoxynucleotide duplexes using catalyzed exchange of the imino proton. *J. Mol. Biol. 200*, 223–238.
52. Leroy, J. L., Charretier, E., Kochoyan, M., and Gueron, M. (1988) Evidence from base-pair kinetics for two types of adenine tract structures in solution: their relation to DNA curvature. *Biochemistry 27*, 8894–8898.
53. Kochoyan, M., Leroy, J. L., and Gueron, M. (1990) Processes of base-pair opening and proton exchange in Z-DNA. *Biochemistry 29*, 4799–4805.
54. Snoussi, K., and Leroy, J. L. (2002) Alteration of A•T base-pair opening kinetics by the ammonium cation in DNA A-tracts. *Biochemistry 41*, 12467–12474.
55. Varnai, P., Canalia, M., and Leroy, J.-L. (2004) Opening mechanism of G·T/U pairs in DNA and RNA duplexes: a combined study of imino proton exchange and molecular dynamics simulation. *J. Am. Chem. Soc. 126*, 14659–14667.
56. Leroy, J. L., Gao, X. L., Misra, V., Gueron, M., and Patel, D. J. (1992) Proton exchange in DNA-luzopeptin and DNA-echinomycin bisintercalation complexes: rates and processes of base-pair opening. *Biochemistry 31*, 1407–1415.
57. Leroy, J. L., Bolo, N., Figueroa, N., Plateau, P., and Gueron, M. (1985) Internal motions of transfer RNA: a study of exchanging protons by magnetic resonance. *J. Biomol. Struct. Dyn. 2*, 915–939.
58. Snoussi, K., and Leroy, J. L. (2001) Imino Proton Exchange and Base-Pair Kinetics in RNA Duplexes. *Biochemistry 40*, 8898–8904.
59. Cahen, P. (2000) Ph.D. Thesis, Université Libre de Bruxelles, Brussels, Belgium.
60. Fasman, G. D. (1975) Handbook of Biochemistry and Molecular Biology , Vol. 1: Nucleic Acids., 3rd ed., CRC Press, Cleveland, OH.
61. Petersheim, M., and Turner, D. H. (1983) Base-stacking and base-pairing contributions to helix stability: thermodynamics of double-helix formation with CCGG, CCGGp, CCGGAp, ACCGGp, CCGGUp, and ACCGGUp. *Biochemistry 22*, 256–263.
62. Plateau, P., and Gueron, M. (1982) Exchangeable proton NMR without base-line distorsion, using new strong-pulse sequences. *J. Am. Chem. Soc. 104*, 7310–7311.
63. Gueron, M., and Leroy, J.-L. (1995) Studies of base pair kinetics by NMR measurement of proton exchange. *Methods Enzymol. 261*, 383–413.
64. Phan, A. T., Gueron, M., and Leroy, J. L. (2001) Investigation of unusual DNA motifs. *Methods Enzymol. 338*, 341–371.
65. Schmidt, K. S., Borkowski, S., Kurreck, J., Stephens, A. W., Bald, R., Hecht, M., Friebe, M., Dinkelborg, L., and Erdmann, V. A. (2004) Application of locked nucleic acids to improve aptamer in vivo stability and targeting function. *Nucleic Acids Res. 32*, 5757–5765.
66. Vesnaver, G., and Breslauer, K. J. (1991) The contribution of DNA single-stranded order to the thermodynamics of duplex formation. *Proc. Natl. Acad. Sci. U. S. A. 88*, 3569–3573.
67. Searle, M. S., and Williams, D. H. (1993) On the stability of nucleic acid structures in solution: Enthalpy-entropy compensations, internal rotations and reversibility. *Nucleic Acids Res. 21*, 2051–2056.
68. Bloomfield, V. A., Crothers, D. M. Tinoco, I., Jr. (2000) Nucleic Acids: Structures, Properties, and Functions, University Science Books, Sausalito, CA.
69. Mirau, P. A., and Kearns, D. R. (1984) Effect of environment, conformation, sequence and base substituents on the imino proton exchange rates in guanine and inosine-containing DNA, RNA, and DNA-RNA duplexes. *J. Mol. Biol. 177*, 207–227.
70. Wu, P., Nakano, S.-I., and Sugimoto, N. (2002) Temperature dependence of thermodynamic properties for DNA/DNA and RNA/DNA duplex formation. *Eur. J. Biochem. 269*, 2821–2830.
71. Patel, D. J., Ikuta, S., Kozlowski, S., and Itakura, K. (1983) Sequence dependence of hydrogen exchange kinetics in DNA duplexes at the individual base pair level in solution. *Proc. Natl. Acad. Sci. U. S. A. 80*, 2184–2188.
72. Leijon, M., and Graeslund, A. (1992) Effects of sequence and length on imino proton exchange and base pair opening kinetics in DNA oligonucleotide duplexes. *Nucleic Acids Res. 20*, 5339–5343.
73. Dornberger, U., Leijon, M., and Fritzsche, H. (1999) High base pair opening rates in tracts of GC base pairs. *J. Biol. Chem. 274*, 6957–6962.
74. Gueron, M. Leroy, J. L. (1992) Base-pair opening in double-stranded nucleic acids, in Nucleic Acids Mol. Biol. (Eckstein, F., Lilley, D. M. J., Eds.) pp 1−22, Springer-Verlag, Berlin.
75. You, Y., Moreira, B. G., Behlke, M. A., and Owczarzy, R. (2006) Design of LNA probes that improve mismatch discrimination. *Nucleic Acids Res. 34*, e60/1–e60/11.
76. Giudice, E., and Lavery, R. (2003) Nucleic acid base pair dynamics: the impact of sequence and structure using free-energy calculations. *J. Am. Chem. Soc. 125*, 4998–4999.